

# Detection of Pneumonia from Chest X-ray Images using Machine Learning

by

Afsana Rahman Priya

19301181

Kashmira Sarkar

19101139

Tania Rahman Khan

19101513

Sohani Fatehin Turna

19301132

Sadia Mubashshira

19101664

A thesis submitted to the Department of Computer Science and Engineering  
in partial fulfillment of the requirements for the degree of  
B.Sc. in Computer Science

Department of Computer Science and Engineering

Brac University

May 2023

© 2023. Brac University  
All rights reserved.

# Declaration

It is hereby declared that

1. The thesis submitted is my/our own original work while completing degree at Brac University.
2. The thesis does not contain material previously published or written by a third party, except where this is appropriately cited through full and accurate referencing.
3. The thesis does not contain material that has been accepted or submitted, for any other degree or diploma at a university or other institution.
4. We have acknowledged all main sources of help.

**Student's Full Name & Signature:**



---

Afsana Rahman Priya  
19301181



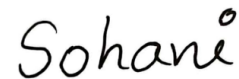
---

Kashmira Sarkar  
19101139



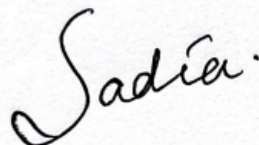
---

Tania Rahman Khan  
19101513



---

Sohani Fatehin Turna  
19301132



---

Sadia Mubashshira  
19101664

# Approval

The thesis titled “Detection of Pneumonia from Chest X-ray Images using Machine Learning” submitted by

1. Afsana Rahman Priya (19301181)
2. Kashmira Sarkar (19101139)
3. Tania Rahman Khan (19101513)
4. Sohani Fatehin Turna (19301132)
5. Sadia Mubashshira (19101664)

Of Spring, 2023 has been accepted as satisfactory in partial fulfillment of the requirement for the degree of B.Sc. in Computer Science and Engineering on May 22, 2023.

## Examining Committee:

Supervisor:  
(Member)



---

Dewan Ziaul Karim  
Lecturer  
Department of Computer Science and Engineering  
Brac University

Program Coordinator:  
(Member)

---

Md. Golam Rabiul Alam  
Professor  
Department of Computer Science and Engineering  
Brac University

Chairperson:  
(Member)

---

Dr. Sadia Hamid Kazi  
Chairperson and Associate Professor  
Department of Computer Science and Engineering  
Brac University

## **Ethics Statement**

The thesis is carefully written in accordance with Brac University policies and regulations as well as the ethical standards for research. In support of our argument, we used data from original sources. We checked to make sure we were properly citing and referencing sources. All five of the paper's co-authors agree to take responsibility for any violations of the thesis code. With the help of a variety of questionnaire-free resources, such as publications and YouTube tutorials, we were able to fix our problems. We also want to take this opportunity to express our gratitude to everyone who has helped us along the way. Our thesis was effectively completed without the use of unethical techniques. The BRAC University's code of ethics governs how we conduct ourselves.

## Abstract

A bacterial infection is the cause of the lung condition known as pneumonia. An essential component of a successful treatment procedure is early diagnosis. Without early diagnosis, pneumonia can be severe or even can cause death. Viewing X-ray images is one of the ways to detect pneumonia. For accurate viewing or reading of X-ray images, a computer-based algorithm is preferable over reading X-ray images manually. In this study, a pneumonia detection system is created using grounded feature extraction from convolutional neural networks (CNN). To predict the occurrence of pneumonia, different classification algorithm models are used. For classification, customized CNN models and various pre-trained models such as VGG-16, Inceptionv3, ResNet50, and VGG-19 are applied to the x-ray image dataset. After implementing all these models we obtained our best accuracy from the Customized CNN model which is 90.43% and the best f1-score from Customized CNN, ResNet50, and VGG-19, the score is 0.87.

**Keywords:** X-ray images; Computer-based algorithm; Customized CNN model; Pre-trained models; VGG-16; Inceptionv3; ResNet50; VGG-19; accuracy; F1-Score

## **Acknowledgement**

First and foremost, we are grateful to Allah SWT for allowing us to complete our thesis without any major setbacks. Then we would especially like to thank our supervisor, Dewan Ziaul Karim, who greatly assisted us in completing our thesis. His guidance and suggestions about the thesis helped us a lot to complete our thesis. Finally, we want to express our gratitude to our parents, without whom we might not have been able to accomplish our aim.

# Table of Contents

Declaration	I
Approval	II
Ethics Statement	III
Abstract	IV
Acknowledgement	V
List of Figures	VIII
List of Tables	IX
Nomenclature	X
<b>1 Introduction</b>	<b>1</b>
<b>2 Problem Statement</b>	<b>2</b>
<b>3 Research Objectives</b>	<b>4</b>
<b>4 Related Work</b>	<b>6</b>
<b>5 Description of Dataset</b>	<b>10</b>
5.1 Dataset Collection . . . . .	10
5.2 Data Augmentation . . . . .	10
5.3 Data Pre-processing . . . . .	11
<b>6 Description of Models</b>	<b>13</b>
6.1 Customized CNN Model . . . . .	13
6.2 VGG16 . . . . .	14
6.3 InceptionV3 . . . . .	15
6.4 ResNet-50 . . . . .	15
6.5 VGG19 . . . . .	16
<b>7 Result and Analysis</b>	<b>17</b>
7.1 Customized CNN Model Outcome . . . . .	17
7.2 VGG16 Model Outcome . . . . .	19
7.3 InceptionV3 Model Outcome . . . . .	22

7.4	Resnet50 Model Outcome . . . . .	25
7.5	VGG19 Model Outcome . . . . .	28
7.6	Comparison of All implemented Models . . . . .	32
<b>8</b>	<b>Conclusion</b>	<b>35</b>
8.1	Conclusion . . . . .	35
8.2	Limitation . . . . .	35
8.3	Future Work Plan . . . . .	35
	References . . . . .	35
	<b>Bibliography</b>	<b>36</b>



# List of Figures

5.1	Dataset image number VS Pneumonia types Bar chart . . . . .	10
5.2	Dataset image number VS Pneumonia types Bar chart after data augmentation . . . . .	11
6.1	Customized CNN model architecture. . . . .	14
6.2	VGG16 model architecture. . . . .	15
6.3	InceptionV3 model architecture. . . . .	15
6.4	ResNet50 model architecture . . . . .	16
6.5	VGG19 model Architecture. . . . .	16
7.1	Customized CNN Model train vs validation accuracy graph . . . . .	17
7.2	Customized CNN Model train vs validation loss graph . . . . .	18
7.3	Customized CNN Model confusion matrix. . . . .	19
7.4	VGG16 Model train vs validation accuracy graph . . . . .	20
7.5	VGG16 Model train vs validation loss graph . . . . .	21
7.6	VGG16 Model confusion matrix. . . . .	22
7.7	InceptionV3 Model train vs validation accuracy graph . . . . .	23
7.8	InceptionV3 Model train vs validation loss graph . . . . .	24
7.9	InceptionV3 Model confusion matrix. . . . .	25
7.10	ResNet50 Model train vs validation accuracy graph . . . . .	26
7.11	ResNet50 Model train vs validation loss graph . . . . .	27
7.12	ResNet50 Model confusion matrix. . . . .	28
7.13	VGG19 Model train vs validation accuracy graph . . . . .	29
7.14	VGG19 Model train vs validation loss graph . . . . .	30
7.15	VGG19 Model confusion matrix. . . . .	31
7.16	Accuracy Comparison bar chart of all Models. . . . .	33
7.17	Loss Comparison bar chart of all Models. . . . .	34

# List of Tables

7.1	Accuracy and loss comparison Table . . . . .	32
7.2	Macro Precision, Recall, F1 Score comparison Table . . . . .	32
7.3	Weighted Precision, Recall, F1 Score comparison Table . . . . .	32

# Nomenclature

The next list describes several symbols that will be later used within the body of the document

$F$  Number of kernels

$P$  Padding amount

$S$  Stride

$W$  Input Size

CXR Chest X-Ray

# Chapter 1

## Introduction

Streptococcus pneumonia, a bacterium that causes pneumonia, is an infectious sickness that can be dangerous and affect the lungs. Pneumonia comes in three primary forms: bacterial, viral, and community-acquired. Mycoplasma, a variety of bacterial pneumonia, generally causes mild respiratory system infections (the corridor of the body involved in breathing). According to encyclopedias, every year, two billion individuals worldwide experience pneumonia. Radiotherapists with advanced training are needed to estimate chest X-rays used to diagnose pneumonia. CAD systems have proven to ease the medical field similar as bone cancer discovery, breast cancer diagnosis using mammograms, lung cancer discovery, etc. thus, there's a critical need for computer-backed opinion(CAD) systems that can help radiologists by snappily relating colorful kinds of pneumonia from Chest X-ray film. The most popular method for diagnosing all types of pneumonia in an individual is to examine areas of the lungs where there is more nebulosity, as shown on a chest X-ray or chest radiograph(CXR). Machine literacy has made significant advancements in the medical industry in terms of a better understanding of illnesses. CNN uses an X-ray image of the chest to assess the possibility of pneumonia and to produce a heatmap that highlights the areas of the image that are most suggestive of the condition. 120 anterior-view chest X-ray pictures from the Chest X-ray 14 collection (Wang et al.[1], 2017) are collectively categorized with over 14 distinct thoracic diseases, including pneumonia. If we set up pneumonia also we further direct the pneumonia type. In relation to the Pneumonia Discovery Challenge, we randomly transform the training dataset, confirmation, and test. There's no case imbrication between the sets. In order to accurately determine whether or not a fresh CXR supplied into the network is pneumonia positive when in the field for individual purposes, we will use CNN, a type of machine literacy trained on normal and pneumonia-positive CXR images.

# Chapter 2

## Problem Statement

Pneumonia is an inflammation generated by a contagion, bacteria, or other germs. There is a potential that pneumonia, whether brought on by bacteria, a virus, or something else, will cause other medical issues. However, they could enter our blood, particularly if we don't seek medical attention if germs were to cause pneumonia. This condition, bacteremia, can result in a catastrophic event known as septic shock. Our lungs can develop pus-filled pockets as a result of pneumonia. Lungs may swell with fluid when someone has pneumonia. If that occurs, they will not be able to adequately oxygenate their blood or remove the carbon dioxide that is already there. Because our organs require oxygen to function, it is a dangerous ailment. Organ failure is also a result of pneumonia. Scientists are trying to figure out why 20% of the patients with pneumonia who are hospitalized also have heart problems. Adults, children, those of having medical issues, and smokers are among those who are more likely to get pneumonia. More than one-third of the victims were toddlers. Without a quick diagnosis, pneumonia has the potential to be severe. Chest x-rays are a crucial pneumonia diagnosis tool everywhere in the world. To correctly interpret the X-ray images, however, specialized expertise and experience are required. As a result, diagnosing pneumonia by viewing X-ray images can be laborious and inaccurate. Similar obscure in photos can also be seen in a wide variety of other medical disorders, such as lung cancer, extra fluid, etc. Because of this, proper picture reading is often preferred. It is commonly known that computing can accurately and more effectively understand X-ray images, and developing a classification for changing the causes of pneumonia in medical imaging can be helpful. Radiology professionals regard X-ray image analysis to be a vital responsibility. As a result, researchers have suggested a number of computer techniques to analyze X-ray images. Several computer-supported opinion methods have been created to help explain x-ray pictures. However, the data supplied by these technologies is insufficient to assist croakers in deciding. A potential strategy in the realm of artificial intelligence is machine learning. Numerous research workshops have been conducted using machine intelligence to examine chest and lung problems. In order to examine chest sickness, vector quantization and retrogression neural networks have been applied. Another study employed chest radiography pictures to identify lung diseases. Image pre-processing was done using histogram equalization, and classification was done using feed-forward neural networks. Despite the fact that this research operated effectively, there was still room for improvement in the matter of improved delicacy, computative time, and flaw rate. Using chest x-ray pictures, we will apply

deep learning in our study to identify pneumonia. We've collected an x-ray images dataset from kaggle. After all preprocessing, we will apply CNN on the dataset to detect Pneumonia from X-ray reports or to classify them.

# Chapter 3

## Research Objectives

In unfolding nations like Bangladesh, life expectancy is growing. To conserve this life expectation, we need good quality treatment. To ensure the quality of treatment, we can use ultramodern technologies. If we can descry pneumonia complaints at an early stage, we might be suitable to cover the life of a case else, there might be a significant peril. Three main types of pneumonia are given below:

1. **Bacterial pneumonia:** This type of Pneumonia occurs from colorful bacteria. Streptococcus pneumonia is the most common pneumonia which falls under this type. It can happen for many reasons as weakness, lack of water in the body, old age, impurity of blood, and germ attack in the lungs. Although bacterial pneumonia can affect people of all ages, there is a high chance of getting affected by pneumonia for those people who smoke cigarettes or drink alcohol.
2. **Viral pneumonia:** This type of pneumonia occurs from colorful contagions like the flu and one-third of Pneumonia patients suffer from this type of Pneumonia. If someone has viral pneumonia, they may be more susceptible to developing bacterial pneumonia.
3. **COVID-19 pneumonia:** There are a lot of COVID-19 cases associated with this type of pneumonia. Most COVID instances exhibit symptoms such as fever, coughing, and breathing problems. Pneumonia caused by COVID-19 can be the cause of early death. It can cause symptoms including exhaustion, chills, nausea or vomiting, diarrhea, stomach discomfort, muscularity, fever, watery eyes, skin rashes, etc. In addition to pneumonia, COVID-19 individuals who develop it may also have a disorder known as acute respiratory torture pattern. It's a sudden onset complaint that makes breathing difficult.

People who are generally affected by this complaint anyone can get pneumonia. still, the following groups are at the topmost threat

1. Grown-ups periods 65 and Children youngish than age 2.
2. People with certain medical conditions.
3. People who bomb.

#### 4. People who are suffering from COVID-19.

Hence, early discovery of complaints can help to help it. But it's relatively impossible to descry pneumonia conditions in this huge population of Bangladesh by clinicians. We need automated tools for discovery, progress observation, and keeping documents of this huge population.



# Chapter 4

## Related Work

P. Rajpurkar, J. Irvin, K. Zhu, et al.[2], proposed a paper on Pneumonia discovery. They have used the CheXNet technique to detect Pneumonia. For detecting Pneumonia, they aimlessly resolve the dataset into training, confirmation, and test cases. Also, they have resized the images of the training set. This paper illustrates that CheXNet achieves a higher score than the radiologist's normal score for pneumonia detection

In a paper by D. Varshni, K. Thakral, et al.[3], the authors came up with a pneumonia discovery model using Radiotherapists with advanced training needed to estimate chest X-rays to diagnose pneumonia. Thus, it would be profitable for the treatment of the illness to produce an automatic system for treating pneumonia. The author stated that they have resized the original 3- channel images as they wanted to reduce the heavy calculation. They have also used several Pre-trained CNN model variations and their statistical findings for their research. Also, they obtain the delicacy of the proposed model was 0.8002.

The paper by T. Rahman, M.E. Chowdhury, A. Khandakar, K.R. Islam, K.F. Islam, Z.B. Mahbub, M.A. Kadir, and S. Kashem et al.[4], aims to automatically describe pneumonia using digital x-ray images. For their research, they used four different deep convolutional neural networks (CNNs) that had already been pre-trained: Alex Net, ResNet18, DenseNet201, and Squeeze Net. The authors created three grouping schemes. The ChestX- shaft pneumonia database from a website was used by the investigators in this study. The test delicacy was 98 percent for normal and pneumonia kinds, 93.3 percent for normal, bacterial, and viral pneumonia types, and 95 percent was the target delicacy for bacterial and viral pneumonia types.

Nayak, Gourisaria, Pandey, and Rautaray et al.[5], suggested convolutional neural networks (CNNs) of various configurations on a machine learning grounded double bracket problem in 2019 showing impacted X-ray dataset. This paper primarily focuses on presenting the outcomes of colorful simple CNN infrastructures and selecting the visually appealing armature based on optimal corresponding minimal loss and maximum delicacy that can serve as an efficient tool for healthcare professionals and the general public to accurately identify and diagnose various types of pneumonia. The CXRs were gathered from pediatric cases from a hospital between the ages of one and five by Kermany. Thus, the sensitivity = 0.9007 and specificity = 0.9216, both of which are above 90%, are good indicators of how well the model

works in both, being able to correctly identify the majority of positive pneumonia cases as well as rule out the negative cases.

A paper by Gabruseva, Tatiana and Poplavskiy, Dmytro and Kalinin, Alexandr et al.[6], the authors created a computational method based on single-shot sensors, squeeze-and-extermination deep convolutional neural networks, accruals, and multi-task literacy in order to identify pneumonia zones. The suggested method was evaluated in the context of the Pneumonia Detection Challenge hosted by the Radiological Society of North America, yielding one of the challenge's favorable outcomes. The database includes 26684 distinct anterior-view X-ray pictures from patients. The labels assigned by the test set's three independent radiologists and the train set's single expert were intersected to determine the ground truth. Other features of the model were hefty accruals with custom gyration, multi-task learning with global bracket affair, and postprocessing.

The authors Hussain, Altaf and Khan, Abbas and Yar, Hikmat et al.[7], suggested a method to automatically identify chest x-ray pictures. Additionally, they attempted to instinctively categorize pneumonia chest X-ray images by obtaining an advanced accuracy of 99.1% employing Mobile Net deep literacy model in this proposed work. Originally the authors loaded the dataset followed by preprocessing and division of 80% and 20% for training and testing independently. Also, the specified conformation of images known as batches are passed to the model for deep point birth and also these uprooted features are fed to the softmax sub-caste for the bracket, which yields chances according to the defined classes of the training dataset. S.Khobragade used a histogram equalization system for preprocessing and also a neural network for brackets to separate between normal and abnormal lung images. Shin used a deep convolutional neural network for the discovery of lymph and interstitial lung conditions. Eventually, the authors used transfer literacy ways and tuned a pre-trained model for a fairly small dataset which proved to be a veritably effective yielding advanced delicacy as well as lower consumption of time and computational cost. As a result, they set up an accuracy of 96.70%.

Using Mask-RCNN, a deep neural network that combines worldwide and precise information for pixel-level segmentation, the authors of a publication by A K Jaiswal, P Tiwari, et al.[8], proposed a pneumonia detection model. The basic network of the Mask-RCNN has been combined with traditional residual convolutional neural networks, ROIalign as a detector, and bounded box as a regressor to extract the properties of real mortal lungs. Scaling during conclusion and losses has been made easier by the pixel-by-pixel segmentation of the lung ambiguity that the ROI classifier revealed. The lung ambiguity identified by ROI classifier has been segmented pixel by pixel, assisting scaling during conclusion and losses.

In a paper by N Dey, Y Zhang et al.[9], using images from chest x-rays, the scientists developed a model for detecting pneumonia based on a customized VGG19 architecture. Both conventional and threshold-filtered chest radiographs were used to perform this work. The chest radiographic picture collection is classified into healthy and pneumonia classes using the VGG19 network. First, a softmax classifier is used to conduct the experimental assessment. Then, using the Ensemble Feature Scheme, a customized VGG19 network is preferred for experimental evaluation (EFS). EFS combines deep features with hand-crafted features using CWT,

DWT, and GLCM. Several classifiers are used to assess the performance of the customized VGG19 (DT). Greater accuracy is obtained by the VGG19 with RF classifier (95.70%). If the same test is carried out with a threshold filter, the VGG19 with RF classifier has a higher classification delicacy of 97.94%.

The authors of a paper by S.B. Atitallah, M. Driss, and colleagues et al.[10], proposed a method based on a substantiation-based fusion theory that would allow the combining of multiple classifiers to produce more reliable results for disease identification. Implementing the Dempster-Shafer proposition for the detection of pneumonia from chest X-ray pictures is the primary benefit of this suggested study. Among the convolutional neural networks in this collection that have already been trained are VGG16, Xception, InceptionV3, ResNet50, and DenseNet201. To increase the number of photographs in the training dataset and enhance the effectiveness of the suggested classifier, they used a variety of data addition approaches. They evaluated the classifier using several metrics particularity, delicacy, and response time. Their suggested strategy gets 97.5% perfection, 98% recall, 97.8% f1- score, and 97.3% delicacy. The authors contend that by using more learning algorithm procedures in the proposed scheme and comparing the results to other sizable datasets to assess progress, these outcomes could be enhanced.

In a paper by A Sharma, D Raju, S Ranjan et al.[11], the authors suggested a way for applying image processing techniques to find pneumonia shadows in chest X-rays. The Otsu Thresholding approach, which they used to define pneumonia, will help distinguish between normal lung tissue and sections that are infected with the disease. To identify an overgrowth, they compute the area ratio of the normal lung region to the whole lung region. In-house algorithms have been created for lung border recognition and cropping images to remove the stomach area. There are just 40 adult CXR in their dataset. The 5 CXR photos from the dataset were randomly given names for effect observation purposes, and the same 5 CXR images were used for their approach by resizing the images. Image brightness is modified using histogram equalization to improve disparity. The intensified discrepancy helps in the discovery of the pneumonia shadows. Otsu thresholding is utilized to separate the healthy lung tissue from the pneumonia-affected tissue in the lung area. The authors claim that they are focusing on alternative thresholding methods for CXR pictures that could produce superior outcomes.

A model using the well-known convolutional neural network models Xception and Vgg16 for predicting pneumonia was developed by H.M. Unver and published in a study by E. Ayan et al.[12].In this proposed work, they used a dataset conforming to 5856 anterior chest X-ray images. In the collection, there are 1583 photos of normal cases and 4273 images of pneumonia cases. Images ranging in size from 712x439 to 2338x2025 are included in the dataset. They used data addition to avoid overfitting and ameliorate the delicacy. Evaluation criteria like delicacy, perceptivity, particularity, recall, perfection, and f1 score were used to evaluate the presented algorithms. By 0.87% in delicacy, 0.91% in particularity, 0.91% in pneumonia perfection, and 0.90% in pneumonia f1 score, the Vgg16 network performs better than the Xception network. In comparison to the Vgg16 network, the Xception network is more effective at identifying cases of pneumonia. In addition, the Vgg16 network

is more effective at identifying typical situations.

R.Kundu and R. Das, et al.[13], suggested that Pneumonia opinion in chest X-ray film can be done using an ensemble deep learning model. They created a computer-backed opinion system that uses chest X-ray film to detect pneumonia automatically. To conduct their disquisition, they employed two datasets. They have used a weighted average and three CNN models in this research. They also used four assessment criteria to determine the classifier weights. For the first and second datasets their delicacy rate, perceptivity rate, perfection rate, and f1- scores are above 98 percent and 86 percent respectively. In the future, they plan to work on visual discrepancy to increase delicacy.

V.Chouhan, S.KSingh, et al.[14], published a research paper for the detection of Pneumonia on the 13th of September. They want to make it easier for both specialists and beginners to diagnose pneumonia. By using the idea of transfer learning they have proposed a novel deep-learning framework for detecting pneumonia. They used a dataset from a Medical Center. They have used image preprocessing, data augmentation, transfer learning, neural networks, feature extraction, and ensemble classification techniques in their study. They compared their findings to those of other authors who researched on the same dataset and demonstrated that their suggested model provided greater accuracy.

# Chapter 5

## Description of Dataset

### 5.1 Dataset Collection

For this exploration, we've collected a dataset that's accessible at <https://www.kaggle.com/datasets/artiomkolas/3-kinds-of-pneumonia>. The main source of the dataset is <https://data.mendeley.com/datasets/9xkhgts2s6/3>. This dataset combines COVID-19 X-ray images and 15 intimately accessible datasets. This dataset contains 1281 COVID-19 X-rays, 3270 Normal X-rays, 1656 viral pneumonia X-rays, and 3001 bacterial pneumonia X-rays.

From our collected dataset we can also observe the number of images according to Pneumonia types in the given bar chart.

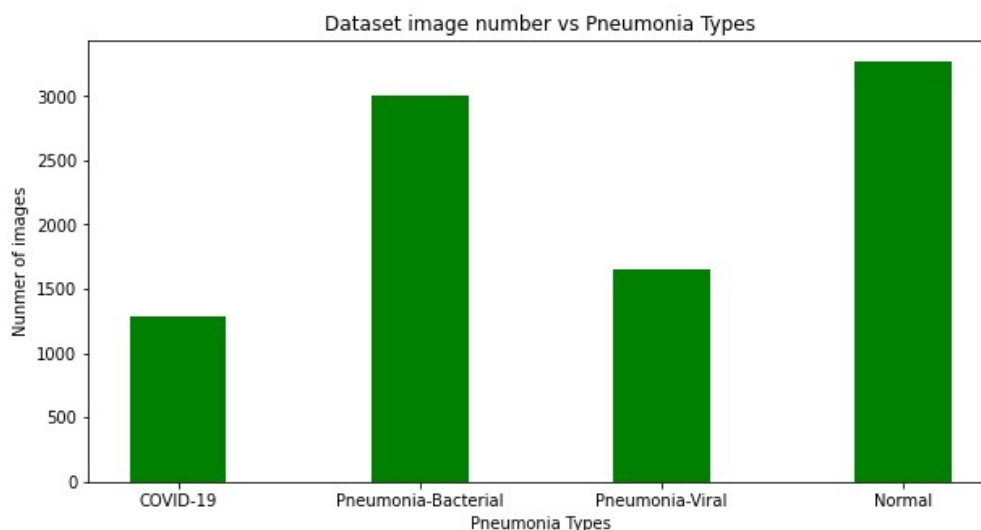


Figure 5.1: Dataset image number VS Pneumonia types Bar chart

### 5.2 Data Augmentation

From the bar chart of Dataset image number VS Pneumonia types, it is obvious that our dataset is not a balanced dataset. For getting good accuracy on any image dataset the number of images is a very important factor. If we increase the number

of images, we will get better accuracy. So, for balancing our dataset and increasing the number we have performed data augmentation. We have randomly picked some pictures and used rotation range = 40, width shift range = 0.2, height shift range = 0.2, shear range = 0.2, zoom range = 0.2, horizontal flip = True, fill mode = 'nearest' on 'Covid-19' and 'Pneumonia-viral' class as these two class has less amount of data.

After data augmentation our updated dataset image numbers according to Pneumonia types are given in the bar chart

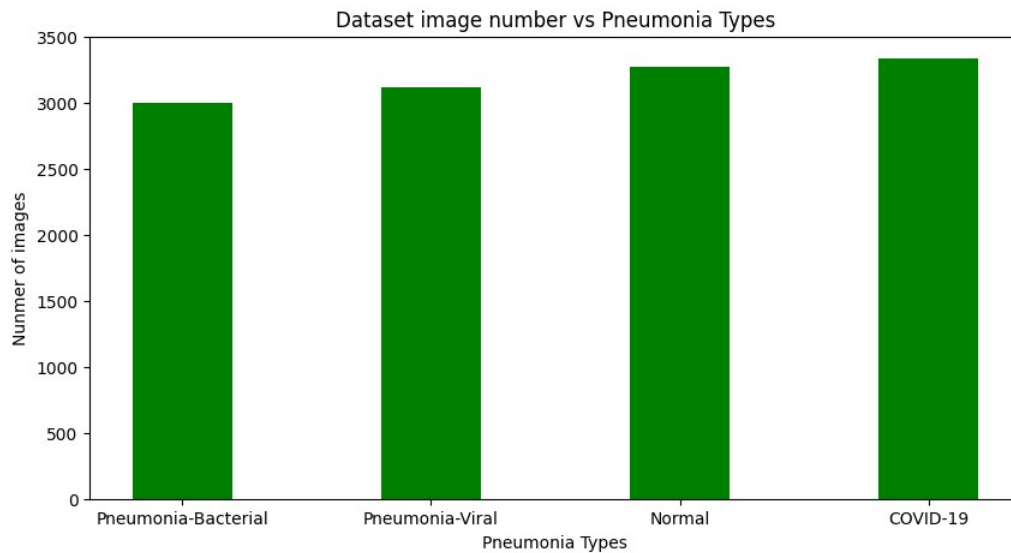


Figure 5.2: Dataset image number VS Pneumonia types Bar chart after data augmentation

### 5.3 Data Pre-processing

For pre-processing the data first of all we have split our dataset. We have a total of 12721 images of four categories after data augmentation. We have split our dataset into a train, valid, and test folder maintaining a ratio of 70%, 20%, and 10%. This splitting gives us 8903, 2543 and 1275 images for train, validation, and testing respectively. After the splitting process, we preprocessed our dataset for further steps.

We have used a customized CNN model and five built-in CNN models of Python Library for our research. For our customized CNN Model we have normalized all images by using  $\text{rescale} = 1/225$  and for the rest of the model we have normalized all images according to the models' pre-processing normalized process so that we can get our result faster. After that, we provided a target detection to all our models which are  $(224 \times 224)$ . We have detected this target because all of our models work on image size  $(224 \times 224 \times 3)$ . Also, we have chosen our batch size of 64 so that every time 64 sample images have been taken by models to update any internal model parameters. We keep the class mode='categorical' as we have 4 images of 4 classes. All these pre-processing are common for train, validation, and testing dataset.

For our train dataset, we have used some more steps of preprocessing. We have used a zoom range of 20% to enlarge the images of the training dataset so that the images of the training dataset become more visible and clear. Then, we used the shear range 20% on our train dataset because the degree-level slant angle is specified by the shear range. Moreover, we have used horizontal flips to make more natural leading lines on the images of the training dataset.

# Chapter 6

## Description of Models

### 6.1 Customized CNN Model

CNN contains layers, including convolution, pooling, and fully connected layers, which make up CNN. Feature extraction is carried out by convolution and pooling layers. By transferring extracted features into the final result, fully connected layers achieve categorization.

#### Customized CNN Model Architecture

1. **Convolutional Layers:** For our customized CNN Model, we have used eleven 2D Convolutional Layers. For our First convolutional layer we used input size (224,224,3) because, in our pre-processing steps, we have resized our images as (224,224). For this layer, our filter size was 64 and we used 'relu' as the activation function and we have kept padding='same'. For the second convolution layer, we used the same filter size which is 64, and the activation function and padding were also the same as the first convolutional layer. In the third and fourth convolutional layers, we used the same activation function and padding but this time our filter size become 128. In the fifth, sixth, and seventh convolutional layers, we used the same activation function and padding but this time our filter size become 256. In the eighth, ninth, tenth, and eleventh convolutional layers, we used the same activation function and padding but this time our filter size become 512. Now, to calculate the size of the output volume the formula is:

$$W_{out} = \frac{W - F + 2 * P}{S} + 1$$

Here,

W x W x D=the size of our input and,

F= with a spatial dimension a Dout number of kernels,

S= stride

P= padding amount

The model uses this formula to obtain its output.



2. **Batch Normalization Layers:** After each convolution layer we have used the Batch Normalization layer. This layer basically normalizes activation which makes our customized CNN Model faster and more stable.
3. **Pooling Layers:** After each batch normalization layer we have used the Pooling layer or Max pooling with padding='same'. This max pool layer basically reduces the computation of our customized CNN Model.
4. **Fully Connected Layers:** After using eleven convolutional, batch normalization, and max pool layers, we have used a flattened layer to fully connect our neural network.
5. **Output Layer:** For getting our output we have added 3 dense layers with units=512 with activation='relu', units=256 with activation='relu', and units=4 with activation='softmax' respectively. Our last dense layer unit=4, as we have 4 categories and activation is 'softmax' to normalize and predict the categories. For compiling our customized CNN model we have used 'adam' optimizer, loss='categorical\_crossentropy', and accuracy metrics.

Our customized CNN Model Structure is given below which will make the structure more understandable. This model has a total of 10402884 parameters, where 10396484 are trainable parameters and 6400 are non-trainable parameters.

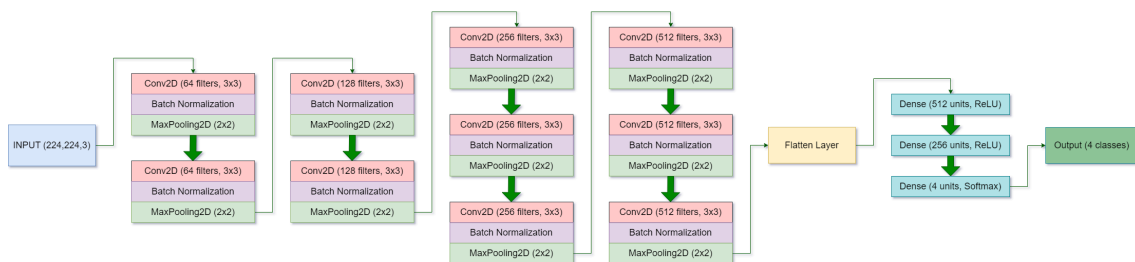


Figure 6.1: Customized CNN model architecture.

## 6.2 VGG16

VGG16 is simple to apply when using transfer learning. In this algorithm, there are in total 21 layers but 16 layers are weighted layers. That's why it's named VGG16. It takes 224\*224-sized images as input and passes through the convolutional and max pooling layers. All the hidden layers of the VGG network apply to ReLU. ReLU is a linear function that, for positive inputs, produces an output that matches the input and, for negative inputs, produces zero. Each convolutional layer produces feature maps and those feature maps' dimensionality and number of parameters are decreased by the pooling layers. VGG uses the softmax function at the end of fully connected layers. To get our output, We have added a flattened layer, and three dense layers with units 512 and 'relu' activation, 256 and 'relu' activation, and 4 with 'softmax' activation respectively.



Figure 6.2: VGG16 model architecture.

### 6.3 InceptionV3

Inception v3 is one of the image identification techniques. The Inception V3 dataset was trained on the original ImageNet dataset, which produced one thousand classes. The model is the outcome of multiple ideas that different researchers have developed over time. This model includes forty-eight total layers. It adds 1x1 convolution before 3x3 convolution because of reducing the number of dimensions as we want to use fewer computation resources. The number of parameters in this model is decreased by factoring into smaller convolutions. The factorization of this model results in asymmetric convolutions such as one 3x3 convolution to two 1x3 and 3x1 convolutions. However, this method’s effectiveness is simply astonishing.

The inception V3 dataset was trained on the original ImageNet dataset, which produced one thousand classes. The model is the outcome of multiple ideas that different researchers have developed over time. This model includes forty-eight total layers. To get our output, We have added a flattened layer, and three dense layers with units 521 and 'relu' activation, 256 and 'reactivation', and 4 with 'softmax' activation respectively.

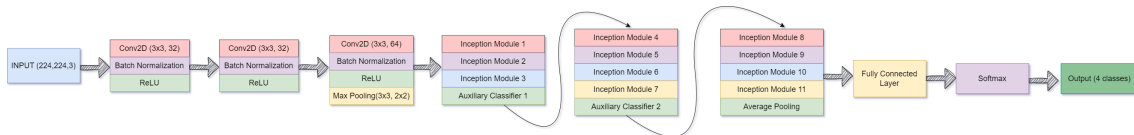


Figure 6.3: InceptionV3 model architecture.

### 6.4 ResNet-50

ResNet-50 has 48 layers of convolution, 1 MaxPool, and 1 Average Pool layer. The Residual Network is called ResNet in short. This model’s key novelty was its ability to train extremely complex neural networks. A robust backbone model called ResNet is often employed in a variety of computer vision tasks. ResNet-50 has 48 layers of convolution, 1 MaxPool, and 1 Average Pool layer. The Residual Network is called ResNet in short. This model’s key novelty was its ability to train extremely complex neural networks. Resnet convolutional neural networks introduce the solution of vanishing gradients problem with the help of skip connection. The main task of skip connection is to add the input to the output of the convolutional layers. We always get the output which is  $y = F(x)$  from the input  $x$  in normal networks. But in Resnet, we get  $F(x) + x$  at the output which is the consequence of the skip connection. If the value of  $F(x)$  becomes 0, then we will get the same output as input which will increase the accuracy.

ResNet-50 uses two different types of blocks:

1. Identity Block
2. Convolutional Block

When we receive the identical output as input, we rely on the identity block and then the original input is added to the output. But if we get different output from input then we can not use identity blocks. Instead of the identity block we have to use the convolutional block which will make the output equal to the input. There are two methods through which convolutional block can make the output equal to the input:

1. Padding the input volume
2. Perform  $(1 * 1)$  convolutions

To get our output, We have added a flattened layer, and three dense layers with units 521 and 'relu' activation, 256 and 'reactivation', and 4 with 'softmax' activation respectively.

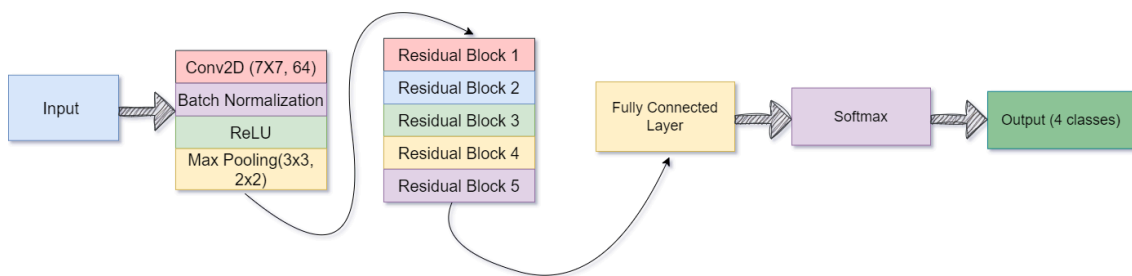


Figure 6.4: ResNet50 model architecture

## 6.5 VGG19

VGG19 is another popular pre-trained image classification model. It takes  $224 * 224$  RGB images as input data and passes through layers. To enhance the accuracy and boost the computational time, RELU which provides non-linearity in the model is used in this model. To get our output, We have added a flattened layer, and three dense layers with units 521 and 'relu' activation, 256 and 'reactivation', and 4 with 'softmax' activation respectively.

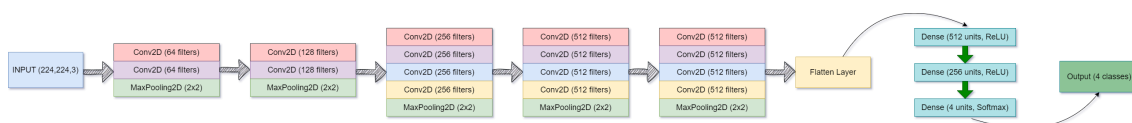


Figure 6.5: VGG19 model Architecture.

# Chapter 7

## Result and Analysis

### 7.1 Customized CNN Model Outcome

We have run 100 epochs for the Customized CNN Model. We used an early stopping process to get minimum loss and maximum accuracy of the validation dataset and we have set patience = 20 for this early stopping process but the model has completed 50 epochs. We have obtained an accuracy of 96.97% and 91.11% on the train set and validation set respectively. On the other hand, we have obtained a loss of 0.0799 and 0.2579 on the train set and validation set respectively. Customized CNN Model Train and Validation dataset accuracy and loss comparing graphs are given below

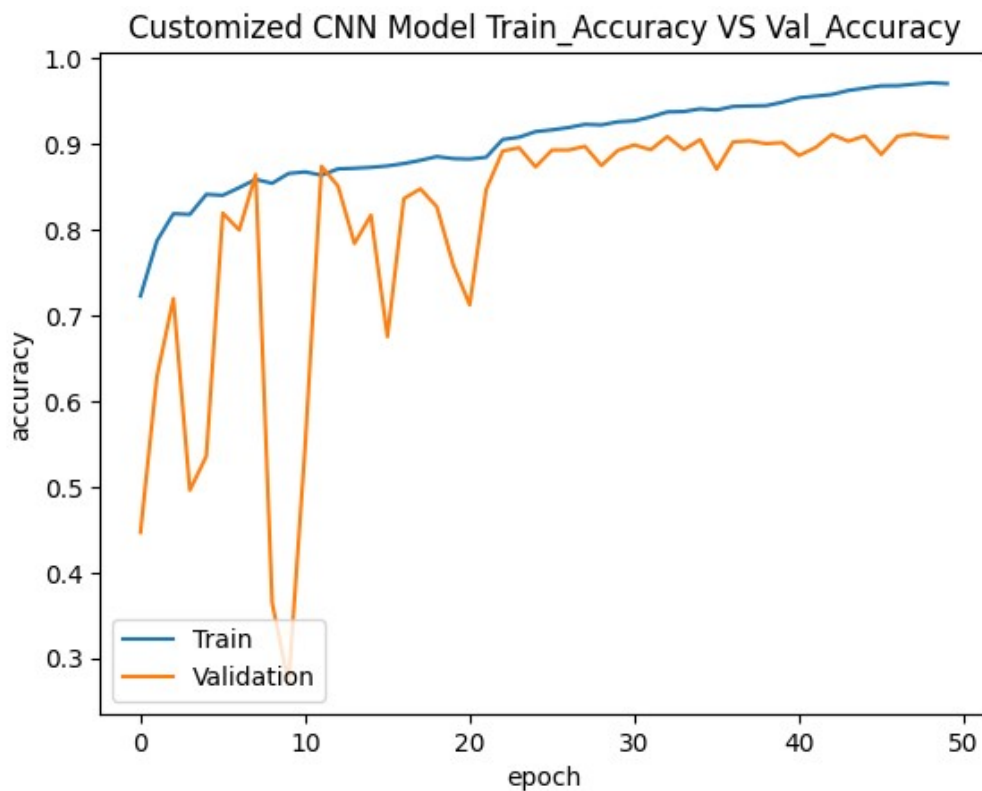


Figure 7.1: Customized CNN Model train vs validation accuracy graph

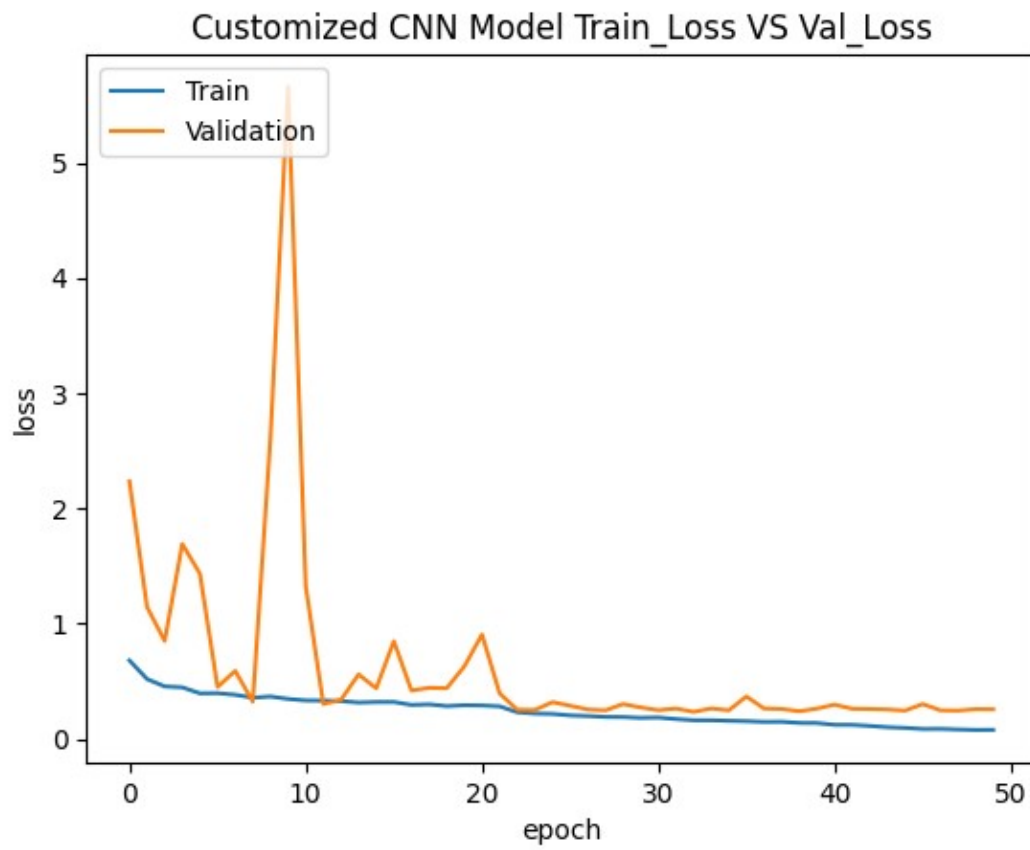


Figure 7.2: Customized CNN Model train vs validation loss graph

We have also performed a confusion matrix on our test set for Customized CNN and the confusion is given below.

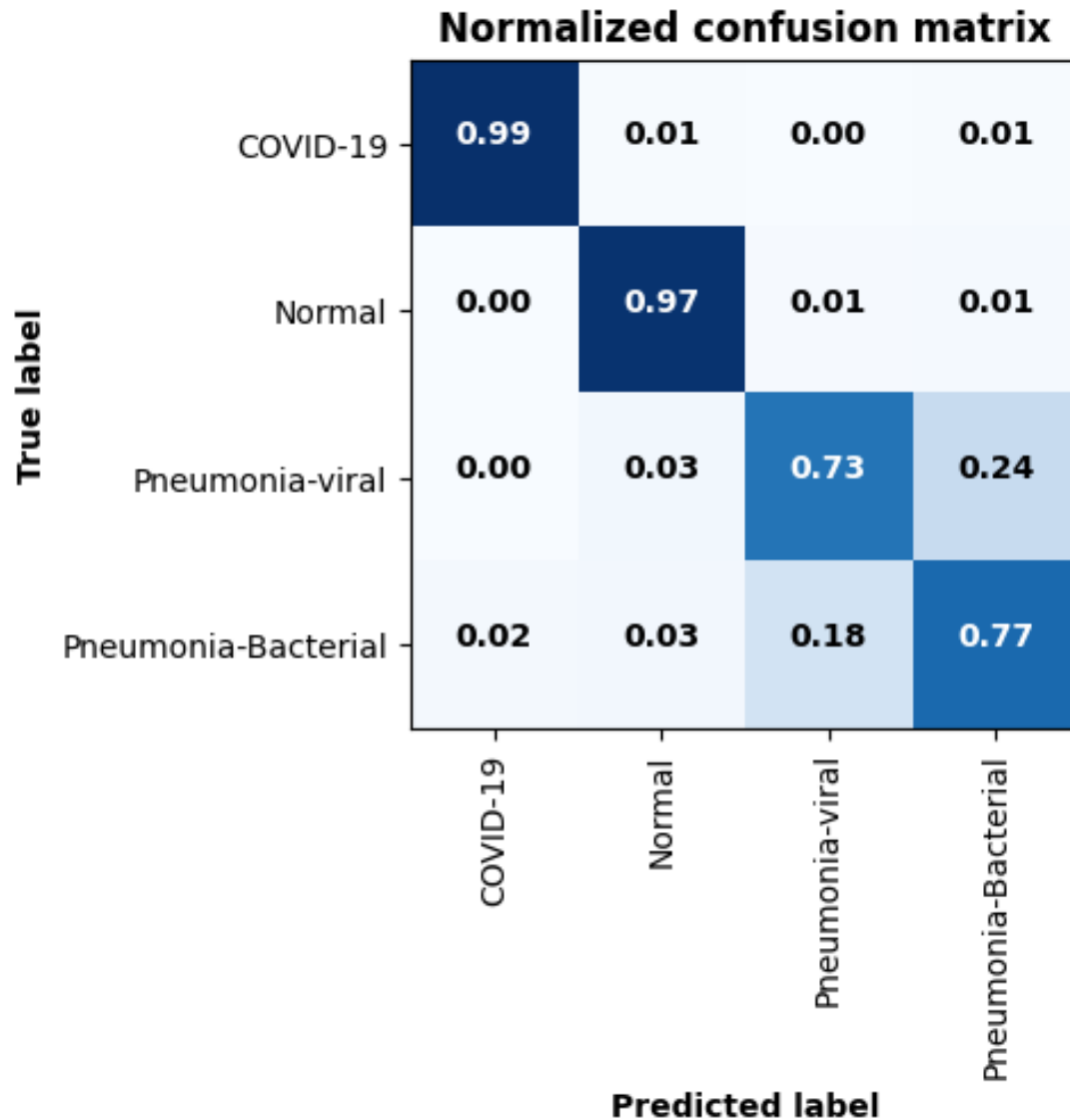


Figure 7.3: Customized CNN Model confusion matrix.

## 7.2 VGG16 Model Outcome

We have run 100 epochs for VGG16 Model. We used an early stopping process to get minimum loss and maximum accuracy of the validation dataset and we have set patience = 20 for the early stopping process. As a result, our VGG16 Model gets its best accuracy after completing 24 epochs. We have obtained an accuracy of 100% and 86.06% on the train and validation set respectively. On the other hand, we have obtained a loss of 0.07 and 1.46 on the train set and validation set respectively. VGG16 Model Train and Validation dataset accuracy and loss comparing graphs are given below.

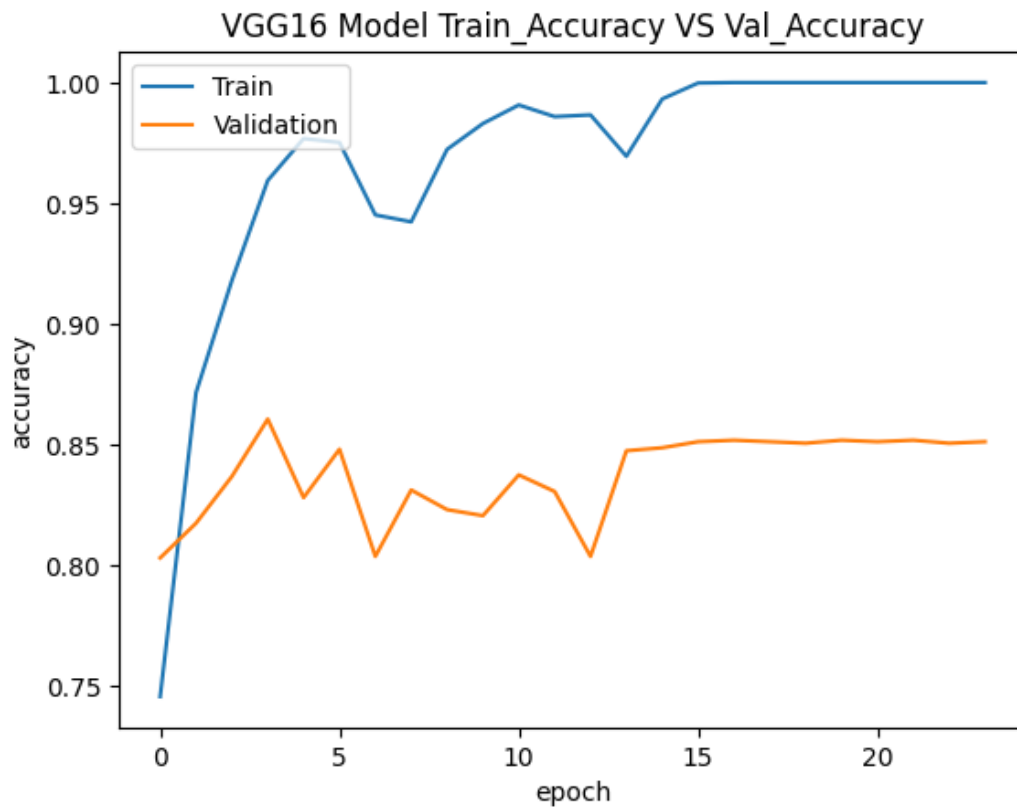


Figure 7.4: VGG16 Model train vs validation accuracy graph

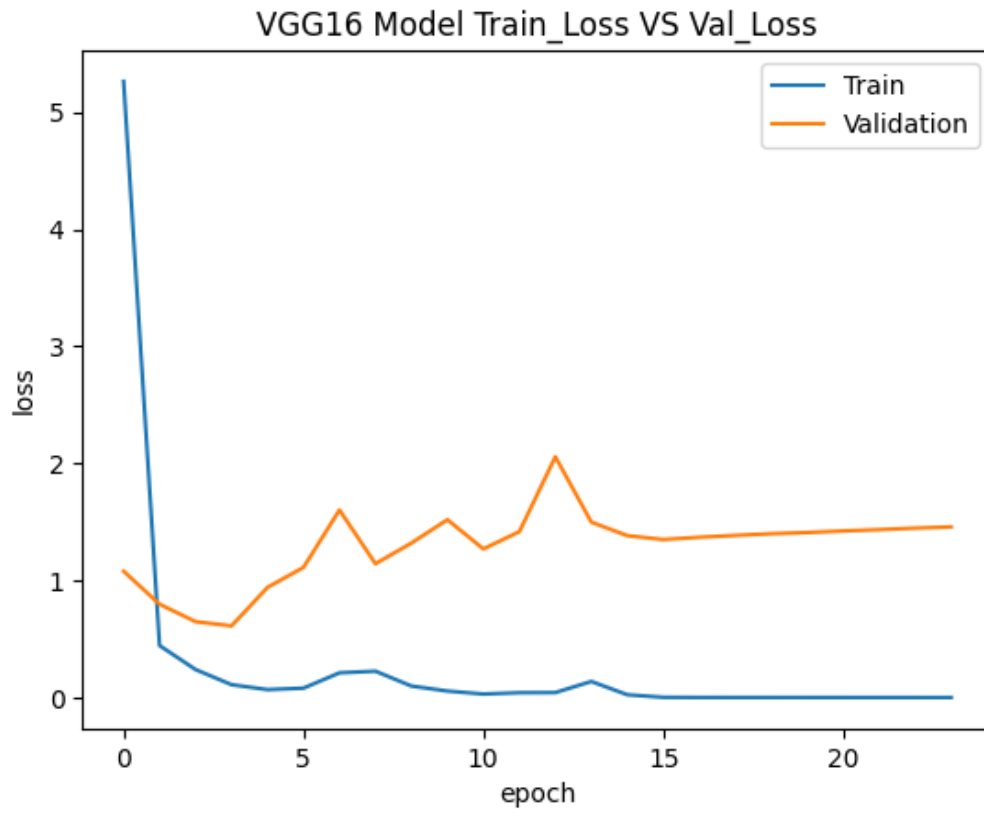


Figure 7.5: VGG16 Model train vs validation loss graph



We have also performed a confusion matrix on our test set for VGG16 and the confusion is given below.

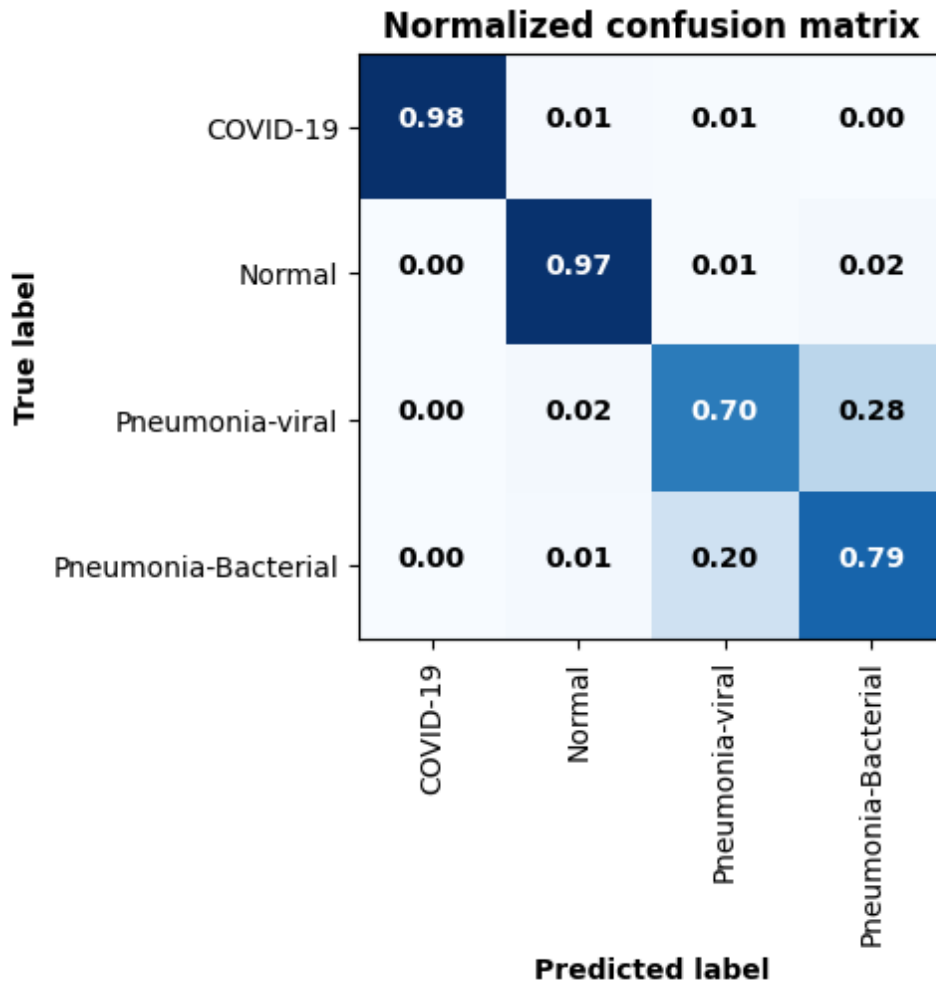


Figure 7.6: VGG16 Model confusion matrix.

### 7.3 InceptionV3 Model Outcome

We have run 100 epochs for InceptionV3 Model. We used an early stopping process to get minimum loss and maximum accuracy of the validation dataset and we have set patience = 20 for this early stopping process. As a result, our InceptionV3 Model gets its best accuracy after completing 29 epochs. We have obtained an accuracy of 100% and 85.13% on the train and validation set respectively. On the other hand, we have obtained a loss of 0.2151 and 1.09 on the train set and validation set respectively. Inceptionv3 Model Train and Validation dataset accuracy and loss comparing graphs are given below.

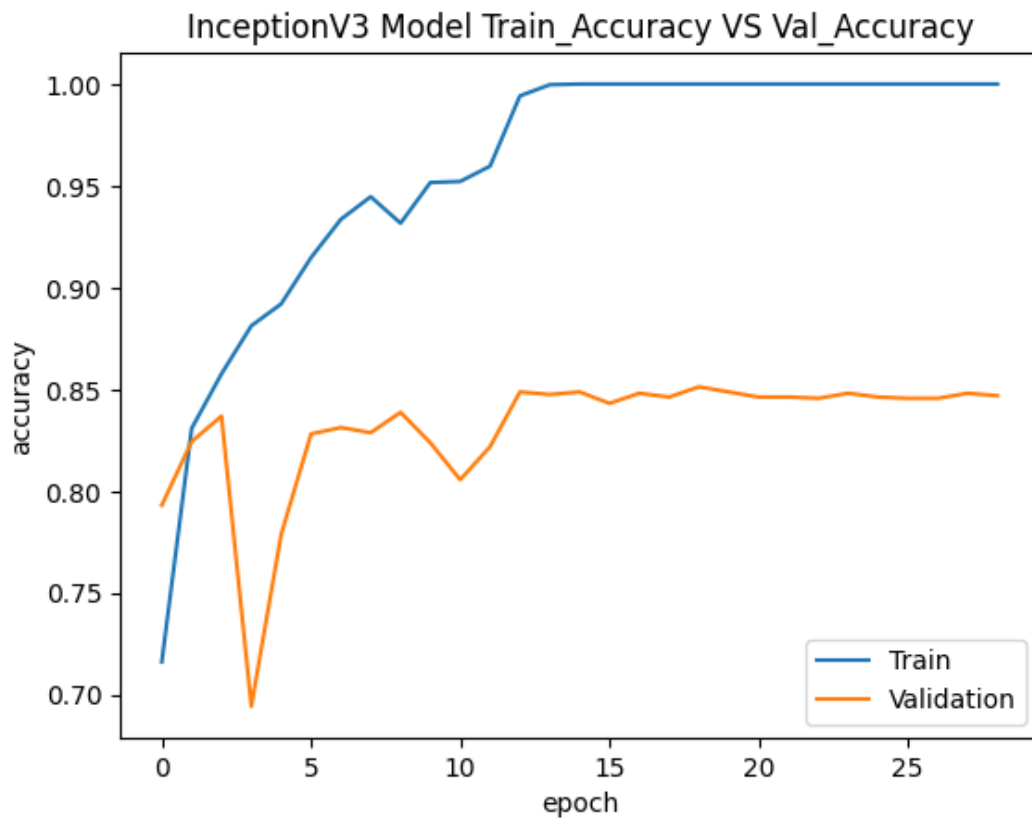


Figure 7.7: InceptionV3 Model train vs validation accuracy graph

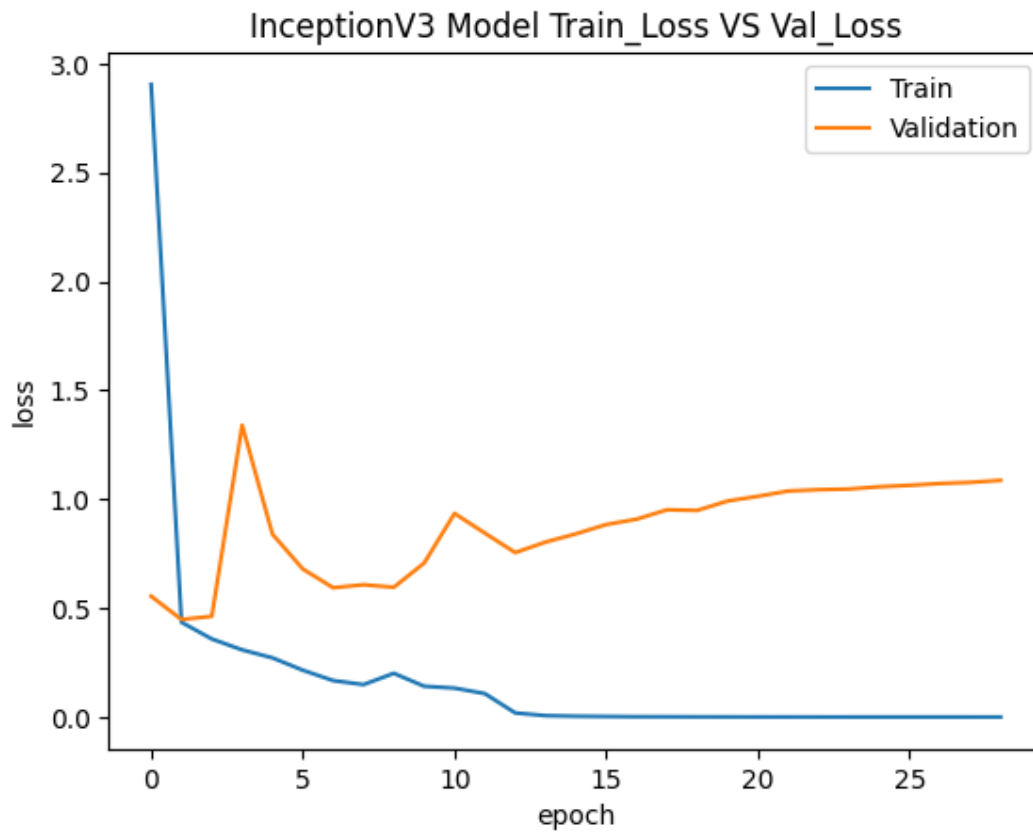


Figure 7.8: InceptionV3 Model train vs validation loss graph

We have also performed a confusion matrix on our test set for Inception V3 and the confusion is given below.

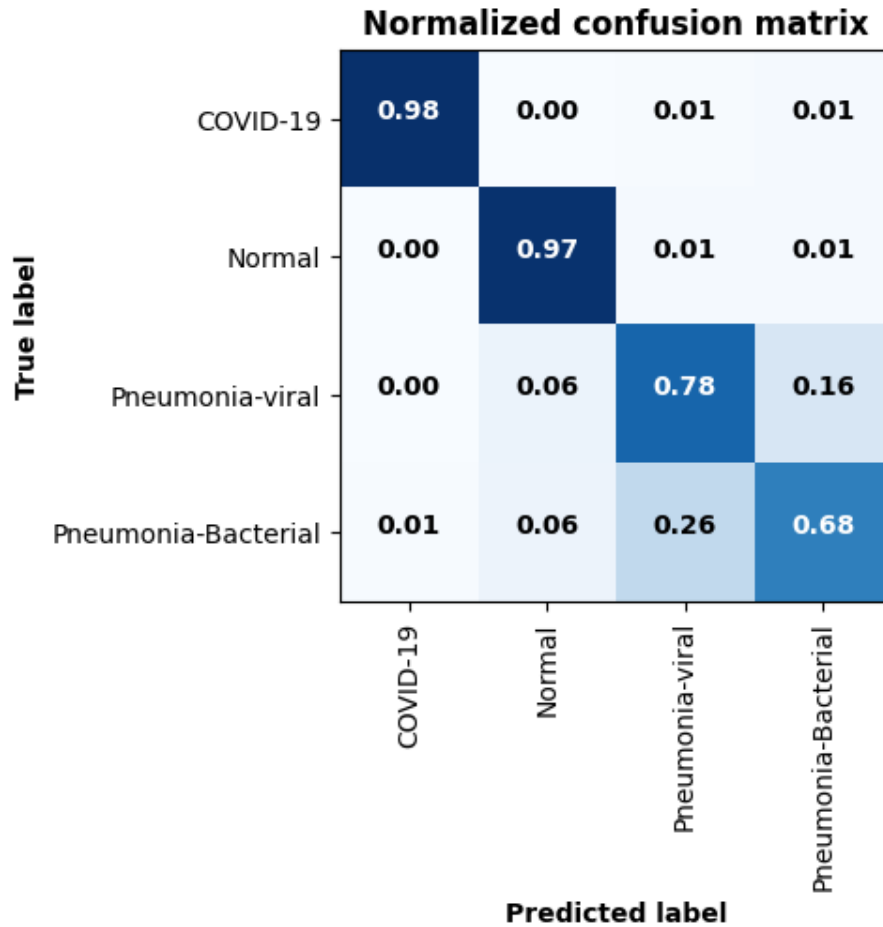


Figure 7.9: InceptionV3 Model confusion matrix.

## 7.4 Resnet50 Model Outcome

We have run 100 epochs for Resnet50 Model. We used an early stopping process to get minimum loss and maximum accuracy of the validation dataset and we have set patience = 20 for this early stopping process. As a result, our Resnet50 Model gets its best accuracy after completing 28 epochs. We have obtained an accuracy of 100% and 87.56% on train and validation respectively. On the other hand, We have obtained a loss of 0.18 and 1.33 on train and validation sets respectively. ResNet50 Model Train and Validation dataset accuracy and loss comparing graphs are given below.

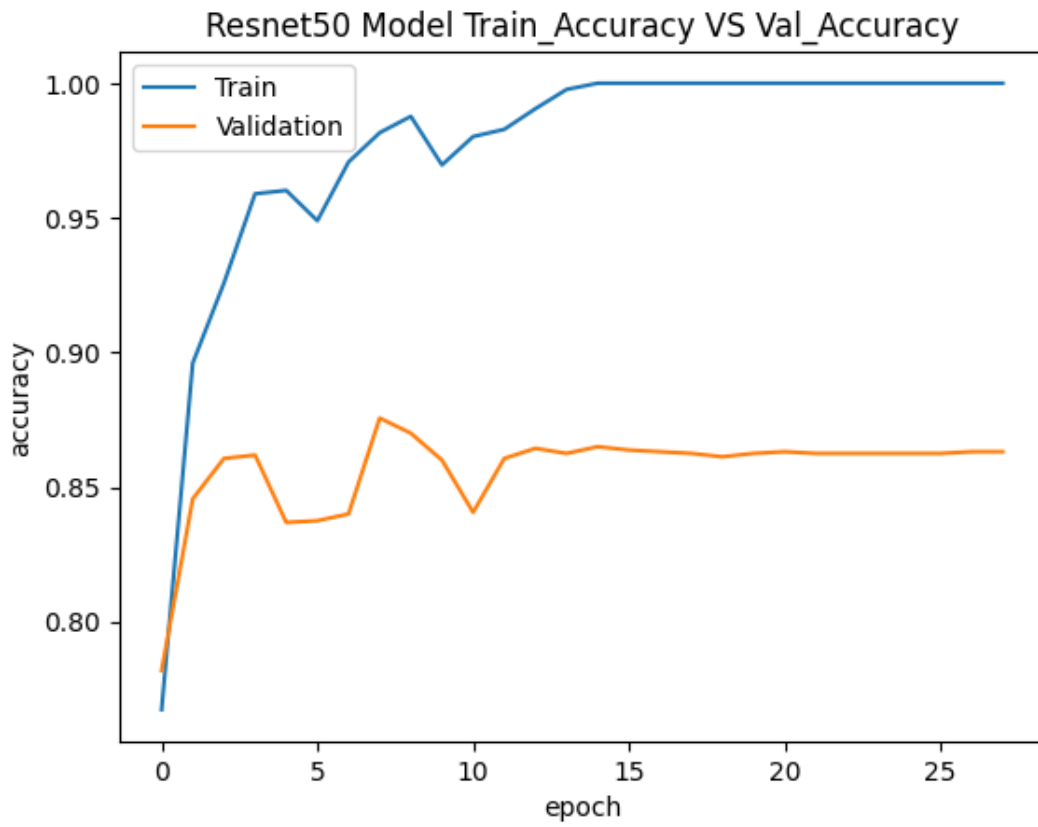


Figure 7.10: ResNet50 Model train vs validation accuracy graph

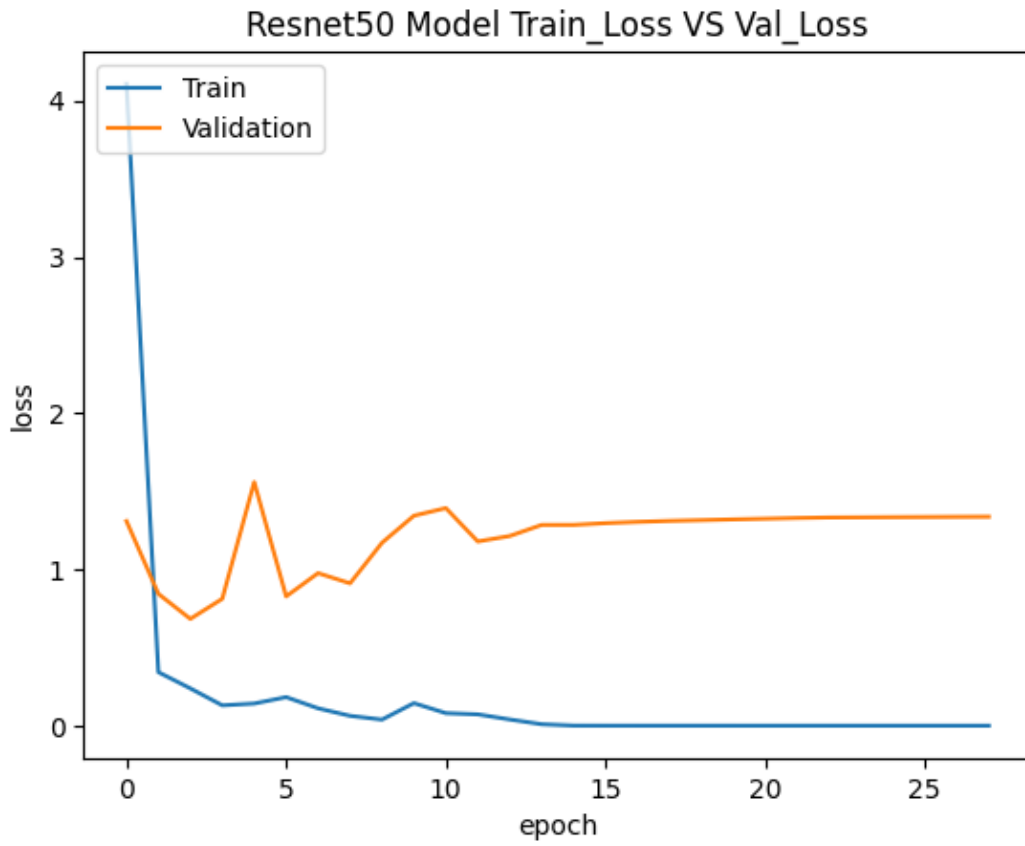


Figure 7.11: ResNet50 Model train vs validation loss graph

We have also performed a confusion matrix on our test set for ResNet50 and the confusion is given below.

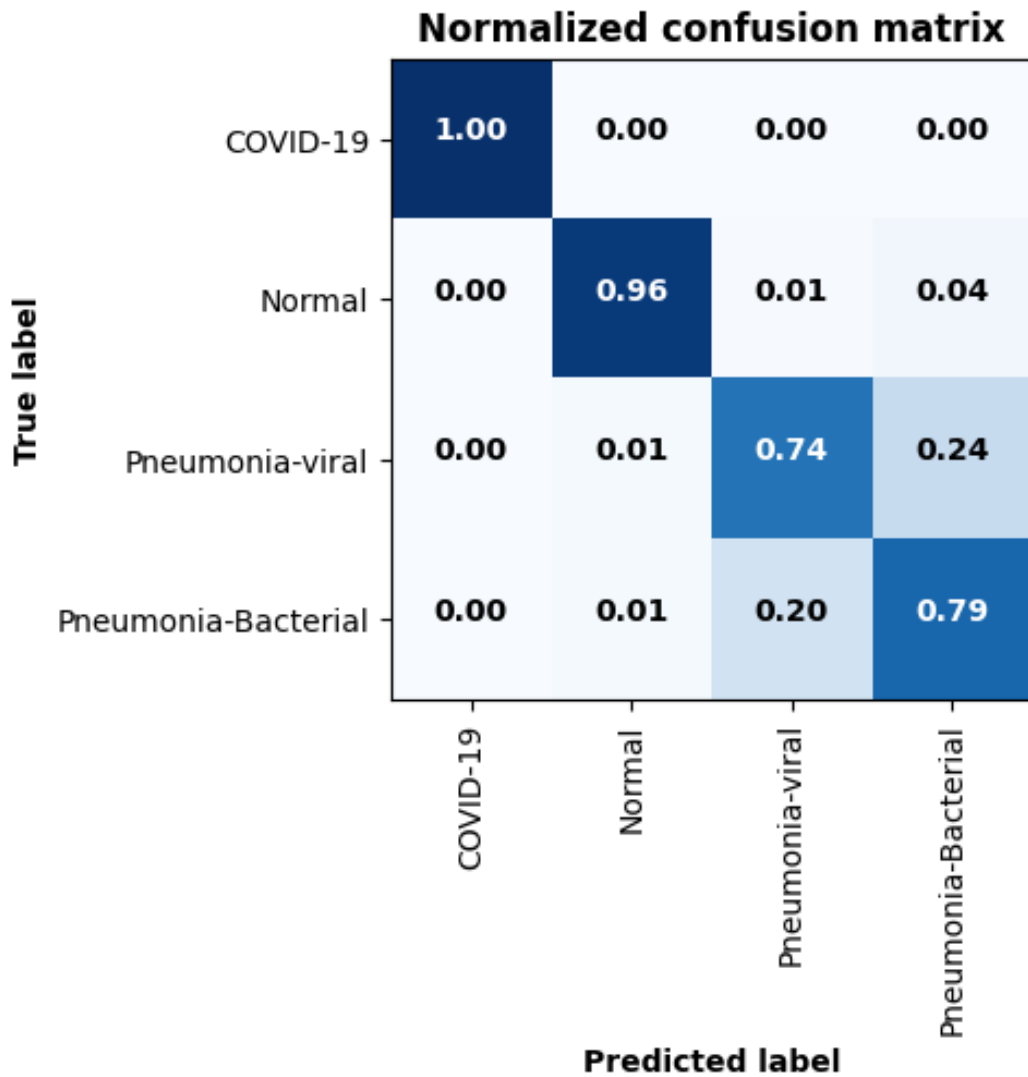


Figure 7.12: ResNet50 Model confusion matrix.

## 7.5 VGG19 Model Outcome

We have run 100 epochs for VGG19 Model. We used an early stopping process to get minimum loss and maximum accuracy of the validation dataset and we have set patience = 20 for this early stopping process. As a result, our VGG19 Model gets its best accuracy after completing 33 epochs. We have obtained an accuracy of 100% 86.50% on train and validation set. On the other hand, We have obtained a loss of 0.07 and 1.45 on the train and validation set. VGG19 Model Train and Validation dataset accuracy and loss comparing graphs are given below.

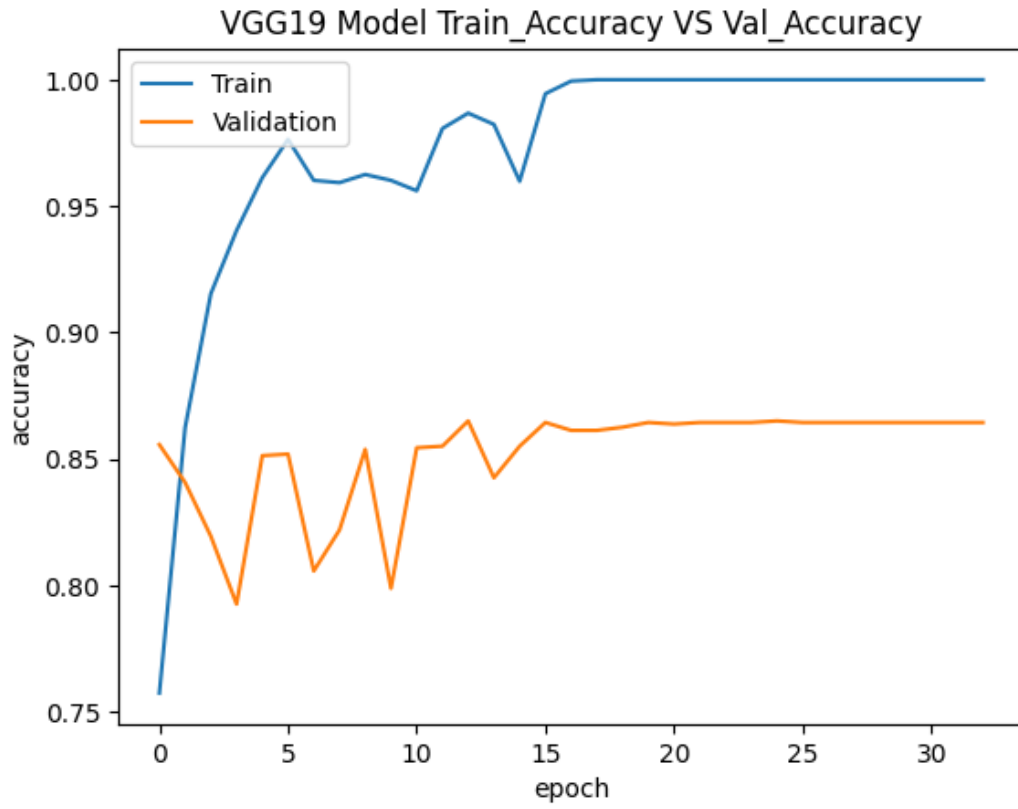


Figure 7.13: VGG19 Model train vs validation accuracy graph



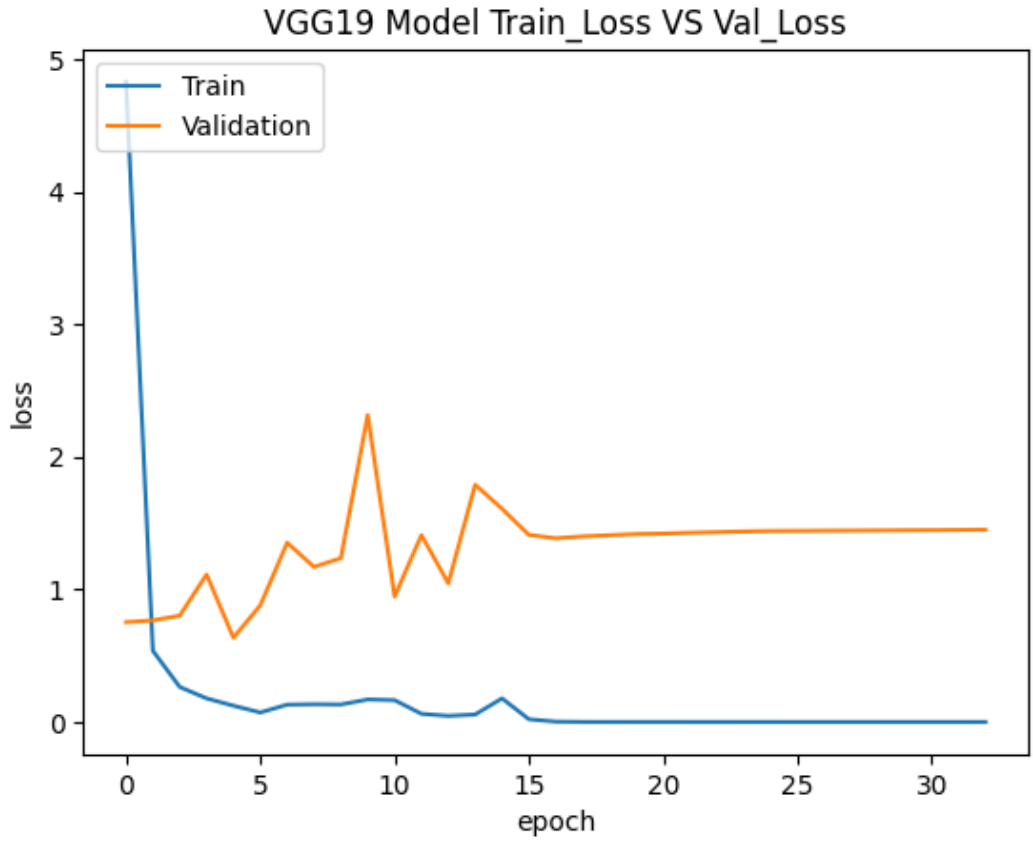


Figure 7.14: VGG19 Model train vs validation loss graph

We have also performed a confusion matrix on our test set for VGG19 and the confusion is given below.

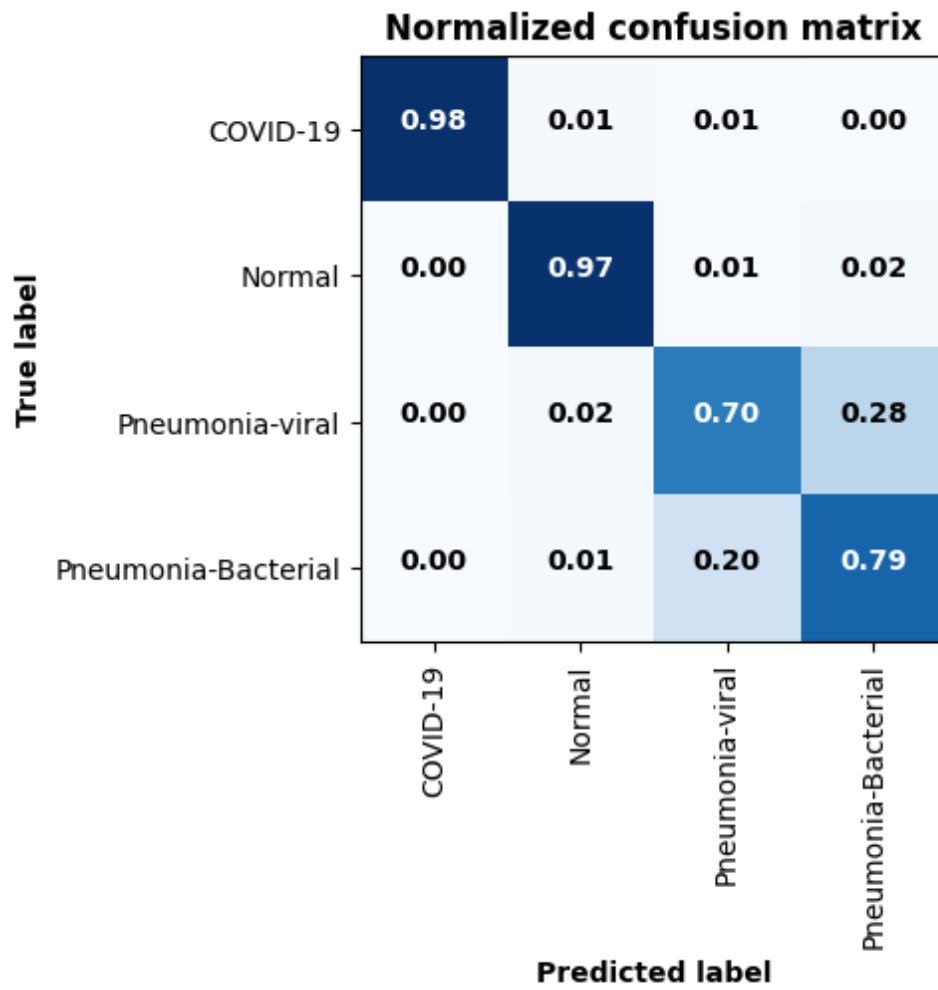


Figure 7.15: VGG19 Model confusion matrix.

## 7.6 Comparison of All implemented Models

Comparison of loss and accuracy of the test set of all the models are given below.

<b>Model Name</b>	<b>Accuracy</b>	<b>Loss</b>
Customized CNN	90.43%	0.29
VGG16	86.12%	0.49
InceptionV3	85.25%	0.98
ResNet50	87.25%	0.89
VGG19	86.62%	0.93

Table 7.1: Accuracy and loss comparison Table

Comparison of macro Precision, Recall, and F1 Score of the test set of all the models are given below.

<b>Model Name</b>	<b>Percision</b>	<b>Recall</b>	<b>F1 Score</b>
Customized CNN	0.86	0.87	0.87
VGG16	0.86	0.86	0.86
InceptionV3	0.85	0.85	0.85
ResNet50	0.87	0.87	0.87
VGG19	0.87	0.87	0.87

Table 7.2: Macro Precision, Recall, F1 Score comparison Table

Comparison of Weighted Precision, Recall, and F1 Score of the test set of all the models are given below.

<b>Model Name</b>	<b>Percision</b>	<b>Recall</b>	<b>F1 Score</b>
Customized CNN	0.86	0.87	0.87
VGG16	0.86	0.86	0.86
InceptionV3	0.85	0.85	0.85
ResNet50	0.87	0.87	0.87
VGG19	0.87	0.87	0.87

Table 7.3: Weighted Precision, Recall, F1 Score comparison Table

We can also observe the comparison from the bar chart of the accuracy and loss of all models.

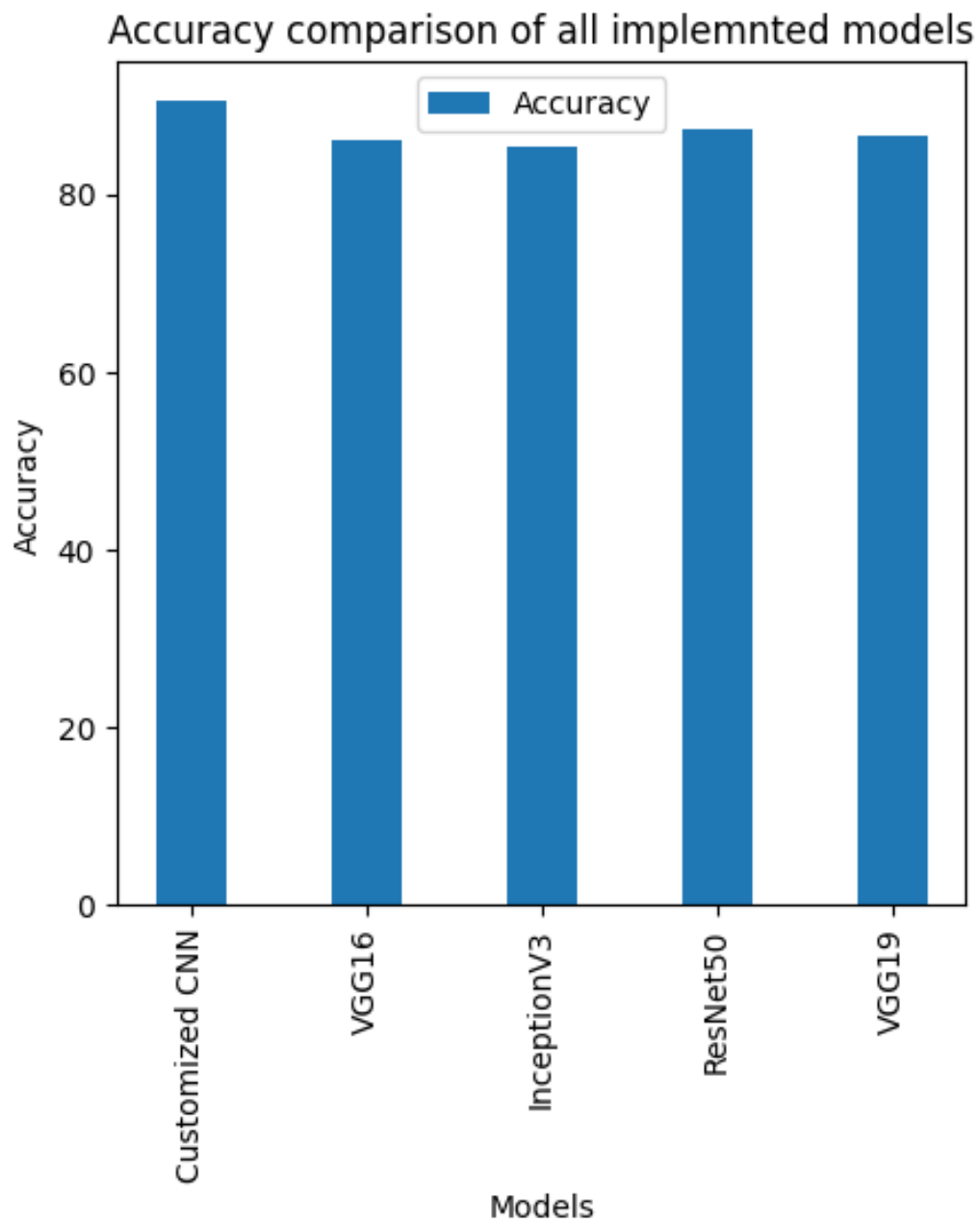


Figure 7.16: Accuracy Comparison bar chart of all Models.

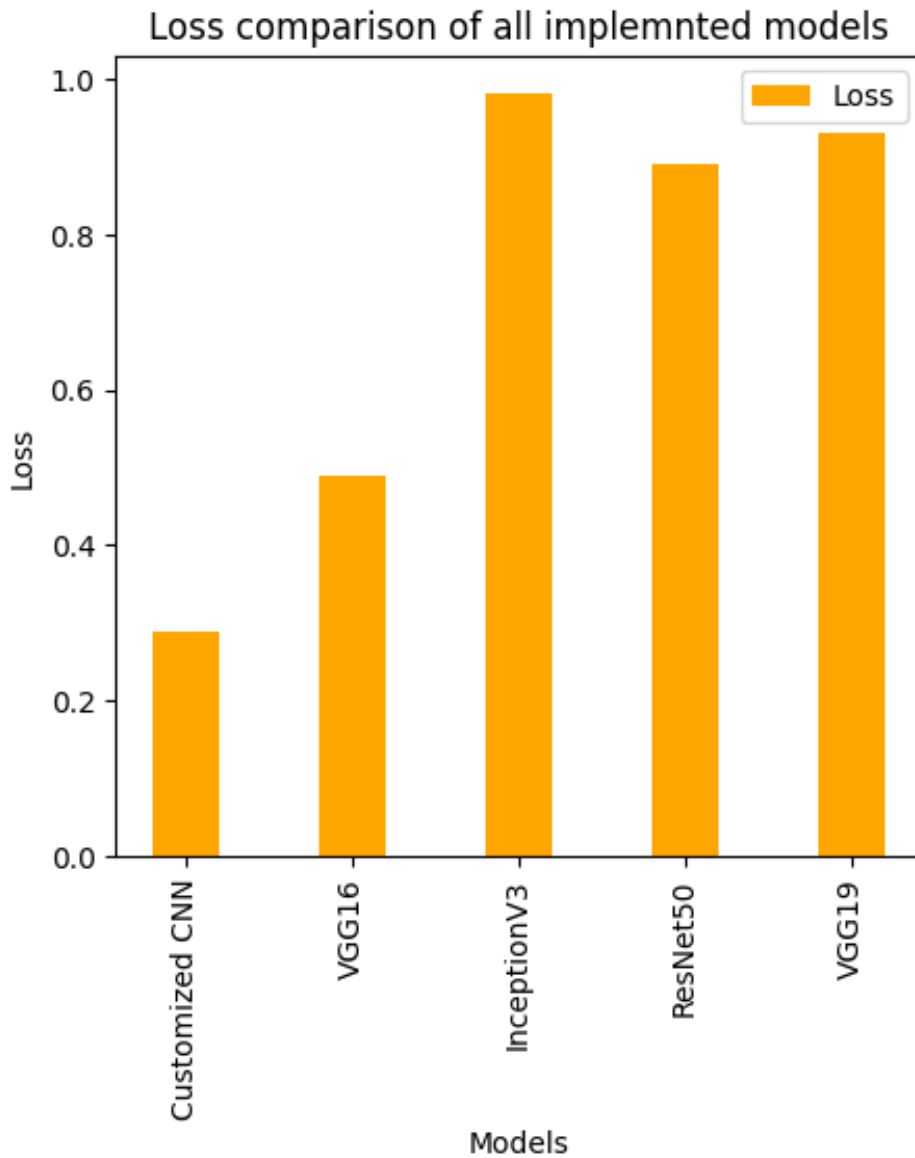


Figure 7.17: Loss Comparison bar chart of all Models.

From the bar chart we can see that all the implemented models are giving us almost the same accuracy but our Customized CNN Model loss is the lowest among all the Models. We are hopeful that if we run our customized CNN Model for more epochs, we will get better accuracy.

# Chapter 8

## Conclusion

### 8.1 Conclusion

To conclude, Pneumonia is very much common in third-world countries. Pneumonia is a bacterial or viral disease of the lung. So, this lung disease can be life-threatening if it is not treated within the proper time. To treat this disease within time, we have to detect it first. The use of chest X-ray reports is widespread for detecting this disease. Sometimes it is very difficult to identify whether the patient really has any Pneumonia disease or not by only using chest X-ray reports. It can happen that the patient does not have any Pneumonia, but the doctor prescribes him/her Pneumonia medicines because of detecting errors in X-ray reports. On the other hand, the patient may have Pneumonia, but the doctor does not treat him/her as a Pneumonia patient because of detecting errors in X-ray reports. As a result, the patient will go through a lot of physical problems because of improper treatment. To detect Pneumonia with less error we have utilized a customized CNN model and some pre-trained models on chest X-ray images which provided good accuracy. If we increase the number of epochs, we will be able to get a more accurate result in detecting Pneumonia. It is our hope that we will be able to identify this disease with fewer errors and with a high degree of precision.

### 8.2 Limitation

As our dataset is an image dataset, running any CNN model takes a lot of time, and with less amount of epochs, the possibility of getting good accuracy is low. If we observe the accuracy graph of all the models, we can see that all the graphs are rising graph. So, it is very clear that if we increase the number of epochs, we will get better accuracy.

### 8.3 Future Work Plan

We want to increase the number of epochs and patience for all models so that we can obtain better accuracy and F1 score later.

# Bibliography

- [1] G. Wang, X. Liu, J. Shen, C. Wang, Z. Li, L. Ye, X. Wu, T. Chen, K. Wang, X. Zhang *et al.*, “A deep-learning pipeline for the diagnosis and discrimination of viral, non-viral and covid-19 pneumonia from chest x-ray images,” *Nature biomedical engineering*, vol. 5, no. 6, pp. 509–521, 2021.
- [2] P. Rajpurkar, J. Irvin, K. Zhu *et al.*, “Chexnet: radiologist-level pneumonia detection on chest x-rays with deep learning available via: <http://arxiv.org/abs/1711.05225> v3,” 2018.
- [3] D. Varshni, K. Thakral, L. Agarwal, R. Nijhawan, and A. Mittal, “Pneumonia detection using cnn based feature extraction,” in *2019 IEEE international conference on electrical, computer and communication technologies (ICECCT)*. IEEE, 2019, pp. 1–7.
- [4] T. Rahman, M. E. Chowdhury, A. Khandakar, K. R. Islam, K. F. Islam, Z. B. Mahbub, M. A. Kadir, and S. Kashem, “Transfer learning with deep convolutional neural network (cnn) for pneumonia detection using chest x-ray,” *Applied Sciences*, vol. 10, no. 9, p. 3233, 2020.
- [5] H. GM, M. K. Gourisaria, S. S. Rautaray, and M. Pandey, “Pneumonia detection using cnn through chest x-ray,” *Journal of Engineering Science and Technology (JESTEC)*, vol. 16, no. 1, pp. 861–876, 2021.
- [6] T. Gabruseva, D. Poplavskiy, and A. Kalinin, “Deep learning for automatic pneumonia detection,” in *Proceedings of the IEEE/CVF conference on computer vision and pattern recognition workshops*, 2020, pp. 350–351.
- [7] A. Hussain, A. Khan, and H. Yar, “Efficient deep learning approach for classification of pneumonia using resources constraint devices in healthcare,” in *Proceedings of the 5th International Conference on Next Generation Computing, Bidholi Via-Prem Nagar, India*, 2019, pp. 20–21.
- [8] A. K. Jaiswal, P. Tiwari, S. Kumar, D. Gupta, A. Khanna, and J. J. Rodrigues, “Identifying pneumonia in chest x-rays: A deep learning approach,” *Measurement*, vol. 145, pp. 511–518, 2019.
- [9] N. Dey, Y.-D. Zhang, V. Rajinikanth, R. Pugalenthi, and N. S. M. Raja, “Customized vgg19 architecture for pneumonia detection in chest x-rays,” *Pattern Recognition Letters*, vol. 143, pp. 67–74, 2021.

- [10] S. Ben Atitallah, M. Driss, W. Boulila, A. Koubaa, and H. Ben Ghézala, “Fusion of convolutional neural networks based on dempster–shafer theory for automatic pneumonia detection from chest x-ray images,” *International Journal of Imaging Systems and Technology*, vol. 32, no. 2, pp. 658–672, 2022.
- [11] A. Sharma, D. Raju, and S. Ranjan, “Detection of pneumonia clouds in chest x-ray using image processing approach,” in *2017 Nirma University International Conference on Engineering (NUiCONE)*. IEEE, 2017, pp. 1–4.
- [12] E. Ayan and H. M. Ünver, “Diagnosis of pneumonia from chest x-ray images using deep learning,” in *2019 Scientific Meeting on Electrical-Electronics & Biomedical Engineering and Computer Science (EBBT)*. Ieee, 2019, pp. 1–5.
- [13] R. Kundu, R. Das, Z. W. Geem, G.-T. Han, and R. Sarkar, “Pneumonia detection in chest x-ray images using an ensemble of deep learning models,” *Plos one*, vol. 16, no. 9, p. e0256630, 2021.
- [14] V. Chouhan, S. K. Singh, A. Khamparia, D. Gupta, P. Tiwari, C. Moreira, R. Damaševičius, and V. H. C. De Albuquerque, “A novel transfer learning based approach for pneumonia detection in chest x-ray images,” *Applied Sciences*, vol. 10, no. 2, p. 559, 2020.